ACS OMEGA

http://pubs.acs.org/journal/acsodf
Article

Cooling of a PVT System Using an Underground Heat Exchanger: An Experimental Study

Saif H. Majeed, Amar S. Abdul-Zahra, Dheya G. Mutasher, Hayder A. Dhahd, Mohammed A. Fayad, Ali H. A. Al-Waeli, Hussein A. Kazem, Miqdam T. Chaichan, Ahmed A. Al-Amiery,* and Wan Nor Roslam Wan Isahak

Cite This: *ACS Omega* 2023, 8, 29926−29938

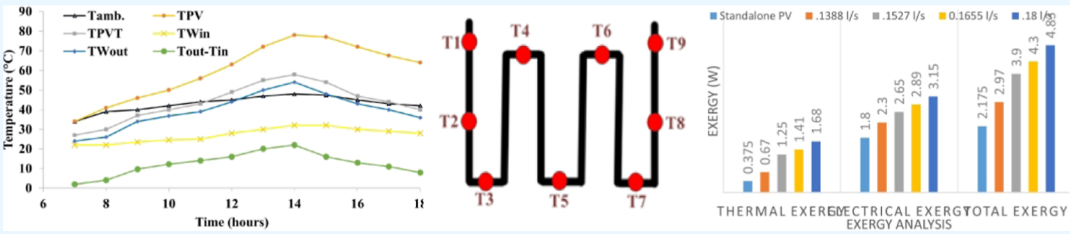

ABSTRACT: In the recent decades, the researchers have been focused on the use of photovoltaic thermal (PVT) systems that provide the best performance and cooling for the photovoltaic panels. In this study, a PVT system consisting of a monocrystalline PV panel and a spiral heat exchanger was connected to an underground heat exchanger that is buried at a depth of 4 m below the surface of the earth. The procedure of the current study can be considered the first of its kind in the Middle East and North Africa region (based on the researchers' knowledge). The study was carried out on agricultural land in Baghdad-Iraq during months of July and August-2022, which are considered the harshest weather conditions for this city. The heat exchanger consists of a copper tube with a length of 21 m and formed in the shape of 3U, and it was buried in the earth and connected with a PVT system. The results of the study showed that the site chosen to bury the heat exchanger (4 m deep) has a stable soil temperature at 22.5 °C. From various volumetric flow rates, a flow rate of 0.18 l/s was selected which is considered the highest flow rate that can show vibration in the PVT system which may harm the system. The practical measurements showed that the largest difference in the surface temperatures of standalone PV and PVT was around 20 °C in favor of the latter. The electrical efficiency of the studied PVT system also increased to outperform the standalone PV system by 127.3%. By comparing the results of the current study with studies of water-cooled PVT systems from the literature, it is clear that the proposed system is feasible and has an acceptable efficiency in such harsh weather conditions tested during the experiment.

1. INTRODUCTION

The excessive consumption of fossil fuels in power plants and transportation is linked to the increase of global warming, melting of large parts of the Arctic and Antarctic, which results in a change in the global climate. Recently, the cold northern countries began to feel the heat of the weather; the snow and rain are also decreased. In contrast, the opposite is in the hot southern countries, where the temperatures have started to decrease in many spots with severe rains causing massive floods, although previously they were suffering from drought.[1] Around 88% of human activities depending on the energy generated from burning fossil fuels, which emits dangerous pollutants to the ground and environment. Among these pollutants, the high concentration of carbon dioxide and methane in the atmosphere is linked to the increase of global warming, which is expected to lead to a catastrophic climate change.[2]

Therefore, the global trend today is to move forward toward the development of alternative energy sources. Solar energy has emerged as one of the fastest growing energy sources in the production of both section electrical energy and thermal energy. It can be considered as a potential alternative that addresses the degradation of energy sources and the problem of climate change. The attention of decision makers has been focused on photovoltaic power plants, and global projects for these plants around the world are increasing.[3] These systems generate 14−20% efficiency and operate with clean energy

Received: December 12, 2022
Accepted: January 9, 2023
Published: August 8, 2023

https://doi.org/10.1021/acsomega.2c07900
ACS Omega 2023, 8, 29926−29938

(free fuel), so they work without pollution. Basically, a system is a group of single modules in parallel and in series. Some environmental factors such as air temperature, sunlight, and dust are contributing in decreasing the module's electrical efficiency.[4] The best areas for installing and operating PV systems are desert areas that do not affect the vegetation cover. However, high temperatures and solar radiation intensity of desert areas are contributing to the decrease in the power generated by PV systems. It is reported that photovoltaic cells absorb the greater part of the solar radiation intensity as heat, which in turn increases their temperature and results in a reduced power yield.[5] During the past 2 decades, the attention of researchers concerned with the impact of cell temperature on its performance has been focused toward new systems consisting of PV modules connected to heat exchangers, commonly referred to as photovoltaic thermal (PVT) systems. These systems can generate electricity and heat together.[6]

A PVT system is an integration of a heat exchanger and a PV module together, where the heat accumulated in the PV panel body is absorbed by the associated collector and dissipated in other applications. In this case, the module cools down and its electrical efficiency improves as well as the heat extracted from it is used as thermal energy.[7] The overall efficiency of such systems is considered high and sometimes reaches more than 90% (not accounting for the difference of energy from—electrical or thermal). The collector used in PVT systems is a heat exchanger whose shape and design depends on the fluid used,[8] water,[9] nanofluids,[10] PCM,[11] or nanofluids and nano-PCM.[12] Hou et al. (2022)[14] also explained that the shape of the flow inside the collector has a key role in determining the enhancement in efficiencies, whether electrical or thermal.

Water is one of the main cooling fluids that has been used for many generations. It has a higher heat capacity than air, which is available and does not cause pollution if it enters the surroundings. Nanofluids differ in their specifications, as they require careful preparations and special care during operation. It must be ensured that they do not leak into the surroundings due to their high cost and the possibility of causing pollution to soil.[14] Nanofluids have higher thermal conductivity than water and have a much more expensive cost than water as well. Therefore, choosing water as a cooling fluid for PVT systems is the better option presently until other fluids are available that has heat storage capacity comparable to water with high conductivity and a lower price.[15]

The availability of water is a problem in the desert lands due to the absence of this source. If water is used in PVT systems, they must be preserved during the cooling process. In addition, the use of cooling towers will cause a waste in both energy and water. Therefore, water cooling by using the shallow near-ground layer can be considered a good way to cool the desert PVT systems and keep an efficient heat transfer process between the cooling water and the soil.[16] Shallow layers of soil maintain stable temperatures throughout the year. The temperature of this layer is usually lower than the summer air temperature and higher than the winter temperature.[17] The fluctuation of the earth's temperature is limited with the change of the seasons, and this fluctuation decreases with the increase in the depth of the layer under the surface of the earth.[18] The deeper layers away from the surface of the earth have higher temperatures, as the soil's temperature at depths from 2 to 3 km with temperature reaches to 25 °C, and reaches to 50 °C at depths greater than 3 km.[19]

The shallow soil temperature is at lower temperatures than the surrounding during summer. This phenomenon increased the chance of using this feature to cool PVT systems by taking advantage of the difference in the temperature. A system consisting of three main parts: PV module with a heat collector and a geothermal heat exchanger (GHE) can make up an excellent PVT system. The difference in temperature will be sufficient to cool the water by dissipating the generated and unwanted heat to the soil.[20] In these systems, the heat accumulated in the body of the PV module is transferred to the water in the heat exchanger that located in its back. Then, this heat is transmitted from the water that circulates inside the tube to the surrounding soil. When adopting such systems, soil properties (components, location, moisture content, and depth) have an important role in determining the PV system thermal performance.[21,22]

The layers of the earth can be divided according to the depth of the soil, the shallower layers are at depths of less than 200 meters, while the deeper layers with a depth of 200 meters which considered medium depth layers. In PVT systems using shallow soil layers, special attention should be paid to the thermophysical properties of the soil being used. The most important of these properties are the soil's heat capacity, thermal conductivity, thermal diffusion, water content, and soil permeability.[23] Furthermore, these properties are formed depending on the soil material origin, the climate of the region, and the soil moisture.[24] Finding these parameters greatly affects the design of geothermal energy pumps as well as soil-cooled PVT systems. The continuous circulation of hot water in the buried pipes inside the soil will cause a clear change in its temperature, especially those adjacent to the pipe, which negatively affects the efficiency of heat transfer and the thermal performance of the buried pipe.[25,26] When using shallow soils for cooling PVT systems, the working fluid must be non-toxic to the soil when it is drained. Therefore, pure water is usually used as a cooling fluid in these systems.[27,28] Parameters such as the heat exchanger inlet temperature and coolant flow rate play an influential role in the overall thermal performance of the system.[29,30]

It is reported that the arrangement of the buried pipes in the soil, the type of material of these pipes, and the geometry of their distribution are the common important factors that affect the performance of underground PVT systems.[31,32] The pipe material and their type selection depends on the type of soil in which the pipes are buried (components and structure). Javadi et al.[28] investigated the thermal GHE system performance focusing on heat flow, thermal resistance, pressure drop, outlet temperature, and heat transfer coefficient. Many researchers found that GHE performance is affected by many factors such as the depth of the backfill, the coolant used, material of the pipes used, and the geometry of the buried pipes. In previous studies[33] and,[34] they confirmed that the soil thermal conductivity is the most important influence in these systems.

The material of buried pipes should be of high specifications such as durability to withstand the pressure of the soil mass and with a long lifespan, as it cannot be filled and replaced every time. Besides, these tubes should also have good thermal conductivity.[35] It is mentioned that there are many types of pipe materials used in the literature. It has been experimented with the use of steel pipes,[36−38] copper,[25,39] and ground pipes in GHE made of polyvinyl chloride (PVC).[40−44] As stated in prior works,[45−47] they used plastic tubes in their experiments, while[48,49] used polyethylene (PE). The last pipe (PE pipe) consists of (60%) polybutylene, then steel (14%) and PVC (8%), and it is one of the most widely used pipes in GHE systems.[41−45] HDPE pipes are currently being adopted in GHEs applications due to their high corrosion resistance despite their low thermal conductivity.

Buried tubes in GHE systems are arranged in two positions, horizontal and vertical. The choice of either of these two modes depends on the conditions of the site on which the station will be located (geography of the site, soil type, and area size). When working in a geothermal system for shallow soil, horizontal pipes are usually deployed at a depth of 1−2 meters below the surface of the earth, and this option is the least expensive to dig and easier to organize and distribute the pipes.[46−49] However, in such systems, there is a need to occupy large areas of land to create better conditions for heat transfer which improves the thermal performance of GHE.[50] When working in a vertical geothermal system, the pipes are buried vertically deep in the soil (sometimes up to 2000 meters) in depths ranging from 50 to 200 meters.[29,51] Selecting this type of system provides better thermal performance when compared with previous methods which require a small land area. However, it is important here to take into account the conditions of the local geological structure, arrangement, and burial of the pipe during work.

The measurements and geometry of the used tube (buried) has a vital role in the system thermal performance. These parameters include the diameter and total length of the pipe, its geometry (flat or helical), the diameter of the solenoid, and the distance between the centers of the coil.[52−55] Also, when groundwater leaks, it causes a form of acceleration in the disposal of accumulated heat around the pipe, and this depends on the homogeneity of the earth surface and the aquifer containing water.[56]

To assess the environmental performance of an earth water heat exchanger PVT system, Choudhary et al.[57] used the Umberto NXT program. From the life cycle assessment, the authors found out that the proposed system consumed more energy during the manufacturing and installation stages. Moreover, the environmental impacts of this system were enormous compared to the regular PV system. On the other hand, the studied system achieved better electrical efficiency than the usual PV system. The earth GHE use with large PVT plants is better in terms of energy production and environmental preservation in comparison with conventional PV plants.

Ruoping et al.[58] conducted a numerical simulation to study a geothermal heat pump (GSHP) attached to a PVT system. Simulation outcomes revealed that the studied system maintained the PV panel temperature at relatively low temperatures with higher electrical efficiency of the studied PVT system in comparison with conventional PV system. The study found a gradual increase in the average soil temperature, after running the system for a long time, ranging from 0.12 to 0.26 °C, annually. Sommerfeldt and Madani[59] studied the combination possibility of using two systems from PVT system connected to a GSHP. The main purpose of this study is to arrive at a system that can provide heating and cooling while generating electricity for sustainable buildings. The current study presented several designs for the proposed system to create an acceptable balance between performance and cost in Sweden.

From the previous review, it is clear that both the ground source heat pump and PVT systems face design and cost challenges, and therefore both have advantages and disadvantages. Combining these two systems in a hybrid cooling PVT system can improve its electrical efficiency, especially in areas with severe weather. In areas with high temperatures and solar radiation intensity, energy must be spent to cool the cooling fluid leaving the PVT system, especially if it cannot be disposed of, as in hot areas or when using high-cost nanofluids. Although there are many studies on PVT systems, very few of them link the cooling of these systems to underground heat exchangers (UHEs). In this study, the aim is to test the practical capabilities of hybrid PVT-UHE technology in very harsh weather conditions in the summer of Baghdad city, Iraq. According to the recent and previous studies, such a study has not been conducted practically or theoretically in the Middle East. There are many difficulties that impede the implementation of such an idea in the city of Baghdad. For example, land prices are very expensive in the capital, Baghdad. Soil properties and quality, which contribute to the sustainability of the system and the perpetuation of a currency for all seasons of the year, must be determined with extreme precision. Also, the drilling and burial operations of the underground system require accuracy in performance and great effort in installing measurement sensors. The preparations for the optimal selection and overcoming these difficulties continued for nearly a year. It should be noted that the authors were unable to find studies similar to such a system to take advantage of the methods used to overcome the difficulties. However, in the literature a large number of studies that used UGE in heating and cooling applications, which were of great help in planning, designing, and supervising the excavation and burial operations for the underground part of the system without losses or errors.

The results of the current study are expected to show promising options in improving the electrical output of PVT systems in regions with harsh weather and the potential to waste the coolant is non-existent with no need for heat absorbed from PV plates. This study will provide a new perspective in the field of research and development for access to PVT-GSHP plants in the desert regions of the Middle East and North Africa.

2. EXPERIMENTAL SETUP

2.1. Study Area. Practical experiments were carried out in Baghdad, which is the capital of Iraq. The administrative area of Baghdad Governorate is 5,159 km^2 (between latitudes 33°10′-33°29′ N and longitudes 44°09′-44°33′ E) with about 24% of the population of Iraq inhabiting the city of Baghdad, making it one of the most densely capitals of the Middle East after Cairo.[60] The climate of Iraq in general is dry and hot in the summer season (the average maximum temperature during this season is 45 °C in the shade) and mild in winter (the average temperature in this season is 14 °C). Approximately, the summer season lasts for about 6 months, while the other three seasons share the remaining 6. In the past 20 years, the country has been subjected to severe drought and a dearth of rainfall, which has significantly increased desertification.[61] This situation made the city prone to many frequent dust storms and the rise of dust continued throughout the years.[62]

Baghdad Governorate is in the middle of the alluvial flood plain of the Tigris and Euphrates rivers. This region also receives high solar radiation intensity, like all regions close to the sun belt. The average intensity of solar radiation ranges from its lowest value 286 W/m^2 (at noon) in winter to its highest value of 890 W/m^2 in summer. The average annual sunshine for the city of Baghdad is 8.7 h/day. The average annual relative humidity and wind speed are around 44.3% and 3.1 m/s, respectively.

The study area is characterized by the availability of groundwater close to the surface of the earth. The people in Baghdad city have used groundwater since ancient times to irrigate crops and drank people and livestock. This area is known as a sedimentary plain, its groundwater is a reservoir close to the surface of the earth at depths of less than 20 m only. Chaichan et al.[63] tested the employment of groundwater with a low salt content in cooling PVT systems. Currently, a growing governmental and popular movement is tending toward photovoltaic power plants as an alternative to fossil fuel power plants. Also, many citizens prefer to replace the local generators with standalone PV systems on the roofs of houses. However, many decision makers and citizens raise fears that PV modules will be affected by high solar radiation and high temperatures, which are continuous most days of the year.[60,64]

2.2. Underground Heat Exchanger Characterizations. In this practical research, the results of Majeed et al.[65] study were used in determining the time and cost of digging and installing an UHE and then burying it. An area of agricultural land was chosen in the city of Baghdad to install and establish the GHE. The area of practical digging was 30 m^2 (6 × 5) m^2, while the depth of drilling was 4 m. The drilling depth was chosen based on Majeed et al.[65] results. Figure 1 illustrates all the drilling process during the experiments. This study proved that at a depth of 4 m was possible to reach a relatively constant ground temperature, which is suitable for efficient heat flow from the PVT system to the soil throughout the year. The UHE was chosen in the form of 3U, with a total length of 22.25 m, inner diameter of 13.41 mm, outside dia. of 15.87 mm, and thermal conductivity of 386 W/m K. It was installed on the floor of the pit (4 m deep) after installing the heat exchangers on it, as Figure 1b showcases. Thermocouples (types K) were used to measure the temperatures. Figure 1c illustrates the thermocouples distribution along the heat exchanger pipes. The pipe material was high thermal conductivity copper tube in this study.

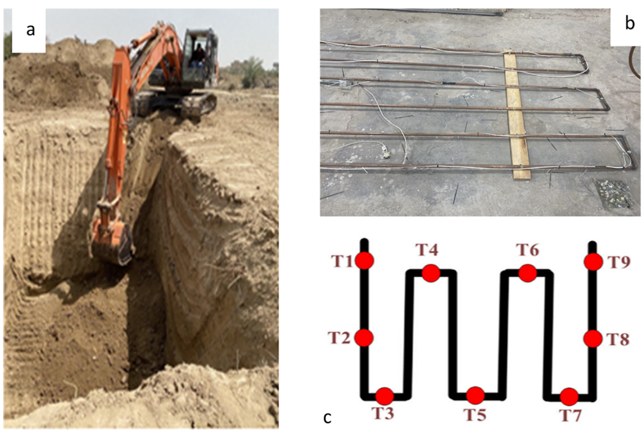

Figure 1. (a) Drilling to the required depth in the study area; (b) the heat exchanger used in test photo; and (c) thermocouple distribution on the UHE.

2.3. PVT System Description. In this study, two PLM-100/12 monocrystalline PV modules oriented at a tilt angle of 33° to the south direction were used in experimental tests. For the modules used, the maximum generated current, voltage, and power are 5.29 A, 19.8 V, and 100 W, respectively. Several thermocouples, (K-type), (with an uncertainty of ±0.87) were fixed to the surface and back of the PV panels. One of the modules was used as a standalone PV system, while the other module back was used to weld a spiral type heat exchanger after painting the welding area with silicone oil to prevent the presence of air gaps between the exchanger and the PV panel. This type of heat exchanger was selected according to the Kazem et al.[66] results.

The tube coming out of the spiral exchanger is connected to a water pump whose cooling water flow is controlled manually by controlling the volumetric flow rate of water entering and leaving the GHE. The flow rate was measured by a US Hunter type sensor with a range of 0.53−80 l/min and an uncertainty of 0.88%. Thermocouples were installed in the HE inlet and outlet to the coil exchanger. Both RHT2 and AT2 are used to measure relative humidity (0−100% RH) with an uncertainty of ±1.2% RH and air temperature (−20 to +80 °C) with an uncertainty of ±1.05 °C, respectively. A BF5 solar sensor was used to measure the intensity of solar radiation due to its capabilities in measuring global and diffuse solar radiation for the radiation intensity range from 0 to 1250 W/m^2 and with an uncertainty of ±0.47. Figure 2a shows a picture of the spiral flow heat exchanger at the back of the PVT system, and Figure 2b illustrates the measurements of the heat exchanger used. A Data Acquisition was used to record multiple measurements and record them on a laptop.

2.4. Pump Selection and Hydraulic Measures. In this study, the capacity and type of the pump were determined before selecting based on hydraulic measurements. In these measurements, many variables (that must be dealt with during the tests) are determined and measured such as pump head, pump efficiency, suction pressure, working hours per day, volume of water required per day, and so forth. The required pumping power was evaluated using the following Al-Simiran[67] equation

$$P_{\text{pump}} = \frac{\rho g(h + \Delta H)Q}{\eta_p \cdot \eta_e} \text{ (kW)} \tag{1}$$

Desired hydraulic energy to operate the study system (cooling water circulation) was calculated adopting the following equation

$$E_h = \eta_s E_{PV} = \rho g h V \eta_s \tag{2}$$

When using a photovoltaic array to equip the pump with the necessary electrical power, the array productivity was calculated using the Kazem et al. equation[68]

$$E_{PV} = A_{PV} \cdot G_T \cdot \eta_{\text{module}} \cdot \eta_{\text{inv}} \cdot \eta_{\text{wire}} \text{ (kW)} \tag{3}$$

To calculate the area of the required PV arrays, the equation was used

$$A_{PV} = \frac{\rho g h V}{G_T \cdot \eta_{PV} \cdot \eta_S} \ (m^2) \tag{4}$$

The total power required to be supplied by the PV array to operate the pump was also calculated by the following equation

$$P_{PV} = \frac{E_h}{G_T \cdot F \cdot E} \text{ (kW)} \tag{5}$$

https://doi.org/10.1021/acsomega.2c07900
ACS Omega 2023, 8, 29926−29938

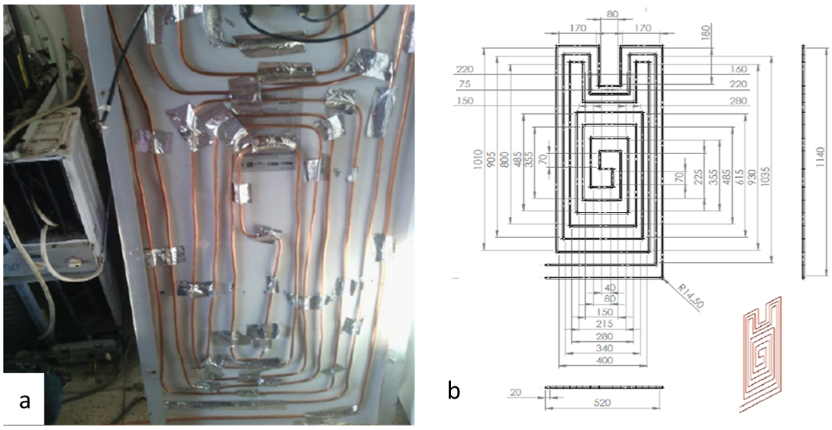

Figure 2. Spiral flow heat exchanger design and configurations; (a) exchanger manufacturing process and (b) exchanger dimensions.

The system efficiency

$$\eta_{\text{system}} = \frac{P_{\text{h}}}{P_{\text{PV}}} = \frac{\rho g h V}{G_{\text{T}} A_{\text{PV}}}\ (\%) \tag{6}$$

By substitution in eq 6, the required pumping power was 1.97 kW h/day. Therefore, the pump required for the experiments must be 140 W. According to eq 5, the required PV array power is 0.6 kW which can be supplied by two PV panels (0.3 kW) connected in series. This pump will work to draw water from the heat exchanger buried at 4 m depth, a constant water level of 3 m, and a dynamic water level of 3.35 m. The circulated water is 4.0 m^3/h with a pumping head of 9 m.

2.5. Data Reduction. The rate of heat transfer per unit length of the buried heat exchanger is calculated by the following Holman equation[69]

$$\grave{Q} = \frac{Q_{\text{heat}}}{L} \tag{7}$$

The rate of useful collected heat (Qu) from the PVT heat exchanger is calculated according to the Niyas et al.[70] equation

$$Q_{\text{heat}} = \dot{m} C_{\text{p}} (T_{\text{in}} - T_{\text{out}}) \tag{8}$$

The electrical efficiency (η_e)

$$\eta_{\text{e}} = \frac{P_{\text{mp}}}{G \cdot A_{\text{module}}} \tag{9}$$

The PV modules' maximum power

$$P_{\text{mp}} = V_{\text{mp}} I_{\text{mp}} \tag{10}$$

Exergy analysis has been considered by many researchers as an important method for determining efficient operating strategy or optimal design in many thermal systems.[71] Therefore, adopting the analysis of external energy in evaluating the performance of thermal systems means not neglecting the kinetic changes on the potential energy. Exergy analysis when heat is available helps in understanding the mechanical work resulting from useful heat and shows the level of energy produced (i.e., high or low level).[72,73]

The general exergy balance[74−76]

$$\sum E_{x_{\text{in}}} - \sum E_{x_{\text{o}}} = \sum E_{x_{\text{d}}} \tag{11}$$

The general exergy balance[74−76]

$$\sum E_{x_{\text{in}}} - \sum (E_{x_{\text{th}}} + E_{x_{\text{pv}}}) = \sum E_{x_{\text{d}}} \tag{12}$$

The input exergy[74−76]

$$E_{x_{\text{in}}} = A_{\text{c}} N_{\text{c}} I \left[1 - \frac{4}{3}\left(\frac{T_{\text{a}}}{T_{\text{s}}} + \frac{1}{3}\left(\frac{T_{\text{a}}}{T_{\text{s}}} \right)^4 \right) \right] \tag{13}$$

The thermal exergy[74−76]

$$E_{x_{\text{th}}} = Q_{\text{u}} \left(1 - \frac{T_{\text{a}} + 273}{T_{\text{o}} + 273} \right) \tag{14}$$

The PV exergy[74−76]

$$E_{x_{\text{PV}}} = \eta_{\text{c}} A_{\text{c}} N_{\text{c}} I \tag{15}$$

The PVT exergy[74−76]

$$E_{x_{\text{PVT}}} = E_{x_{\text{Th}}} + E_{x_{\text{PV}}} \tag{16}$$

The exergy destruction or irreversibility[74−76]

$$E_{x_{\text{d}}} = T_{\text{a}} S_{\text{gen}} \tag{17}$$

The exergy efficiency[74−76]

$$\eta_{\text{ex}} = 1 - \frac{E_{x_{\text{d}}}}{E_{x_{\text{in}}}} \tag{18}$$

2.6. Uncertainty Analysis. Measurements' errors occur in the scales deviate from the standard readings, which negatively affects the accuracy of the results in practical experiments. Hence, the importance of focusing (before the start of the experiments) on calibrating the devices and ensuring the validity of their practical measurements, which increases the reliability of the measurements and the validity of the results obtained. The readings' deviations in the scales resulting from several factors represent the uncertainty affecting the accuracy of the measurement. The difference between the concepts of measurement accuracy and uncertainty must be taken into account. In addition, there are random errors such as human error resulting from the experience and credibility of the examiner himself. Sometimes exaggerated data appear, and in such cases, it is expressed in uncertainty resulting from obvious errors, and the causative factor must be identified and eliminated immediately and the measurements should be re-established. Here, it is important to mention that data that do not meet expectations should not be discarded as bad data. However, when exaggerated or unacceptable measurements are

https://doi.org/10.1021/acsomega.2c07900
ACS Omega 2023, 8, 29926−29938

Table 1. Measuring Devices (Used in This Study) Accuracies and Uncertainties

no.	measurement	device	range	accuracy	uncertainty (%)
1	thermocouples type K		−50 to 150	±2 °C	±0.87
2	flow meter	US hunter	0.53−80 l/min	±0.05 l/min	±0.88
3	relative humidity	RHT2	0−100%	±1.7 RH	±1.2
4	air temperature	AT2	−20 °C to +80 °C	±2 °C	±1.05
5	solar radiation intensity	BF5 solar sensor	0 to 1250 W/m^2	±3 W/m^2	±0.47
6	multimeter (voltage)	AstroAI	0−500 V	±2 V	±0.6
7	multimeter (current)	AstroAI	0−10 Amp	±1.3 amp	±0.73

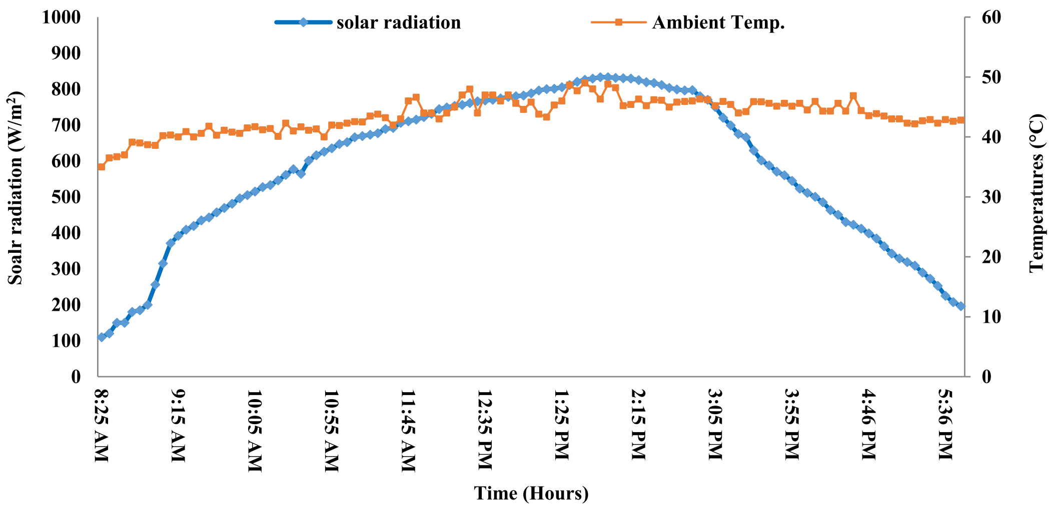

Figure 3. Tests average climatic conditions (ambient temperature and irradiance) during tests period.

obtained under the same condition and the same operating conditions, the measuring devices and measurement method must be checked and re-examined and measured again. Repeatability (repeating experiments several times not less than three) is a very important procedure in practical experiments. It is possible, through repeatability, to neutralize deviation and measurement error to a high degree. Holman [69] concentrated on the importance of preventing human bias from interfering with practical measurements by misusing the concept of "should be".

In the current experiments, the measuring devices used were calibrated and their deviation from the standard values was determined. In the second step, to reach the degree of uncertainty in the results, the following Klein and McClintock (1953) equation was applied

$$W_R = \left[\left(\frac{\partial R}{\partial x_1}w_1\right)^2 + \left(\frac{\partial R}{\partial x_2}w_2\right)^2 + \dots + \left(\frac{\partial R}{\partial x_n}w_n\right)^2\right]^{0.5} \quad (19)$$

WR is the results' total uncertainty, the independent variable for a given function (x1, x2, ..., xn) is represented by R, and the independent variables uncertainties are represented by (w1, w2, ..., wn). Table 1 includes the devices used in the experiments measurements and its uncertainties.

From Table 1, it is clear that the measuring equipment used in the tests has a geometrically acceptable degree of uncertainty, which is less than 3%. To ensure repeatability, the measurements were repeated for each test at least three times and their arithmetic mean was taken.

2.7. Test Procedure. The area chosen for UHE burial adopted Majeed et al.[65] experiments to ensure the optimum conditions for the tests. Experiments were installed in an agricultural land in Baghdad city. The site's soil has a moisture content, which aids in accelerating the process of transferring and dissipating heat from the buried exchanger. The depth was chosen after verifying the temperature of the earth's layers and the validity of this layer to provide a large difference in temperature to accelerate heat transfer. Although the thermal conductivity of water is not high, however, if the temperature difference is large, the heat flow will be greater. Several mass flow rates of circulating water (0.1388, 0.1527, 0.1655, and 0.18) l/s were tested to reach the optimum thermal rate. The mass flow rate did not exceed 0.18 l/s because of the appearance of high vibrations in the PVT system. To prevent the PVT system form damage, experiments were carried out up to this rate (0.18 l/s). Practical experiments were carried out in July and August 2022. These 2 months are considered to be the hottest months of the year with temperatures (exceeding 60 °C on the day time) and solar radiation (the maximum solar radiation intensity measured in the tests was 1216 W/m^2 at 8/8/2022). In Iraq, dust rises in these 2 months; therefore, the solar modules are cleaned daily before the tests to ensure no dust deposition on the system according to the results of Chaichan and Kazem.[64] The practical measurements start at 7 AM in the morning and end at sunset, while the UHE temperatures are recorded and saved throughout the day.

3. RESULTS AND DISCUSSION

In the cold countries of the world, it is important to utilize the heat absorbed from the PV modules and retain it for use in other applications. However, in countries with very high ambient temperatures, the use of this heat is limited. It is necessary to get rid of this heat to achieve the best performance of PVT systems. This concept should be applied

https://doi.org/10.1021/acsomega.2c07900
ACS Omega 2023, 8, 29926−29938

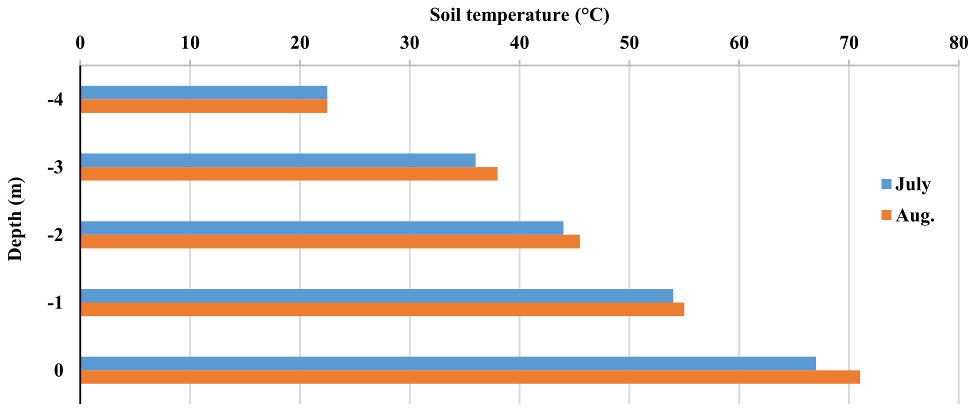

Figure 4. Average soil temperature gradient in the study area during the tests.

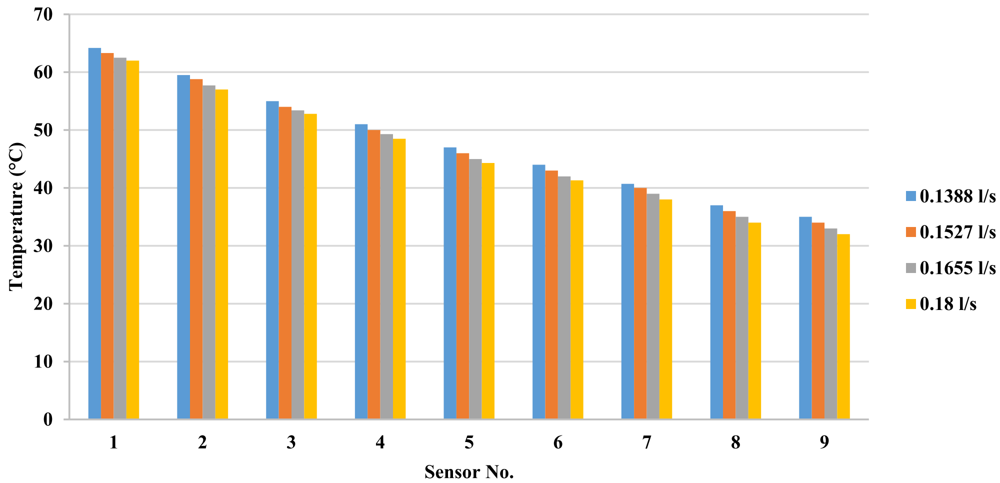

Figure 5. Average temperatures distributed over sensors during morning operation.

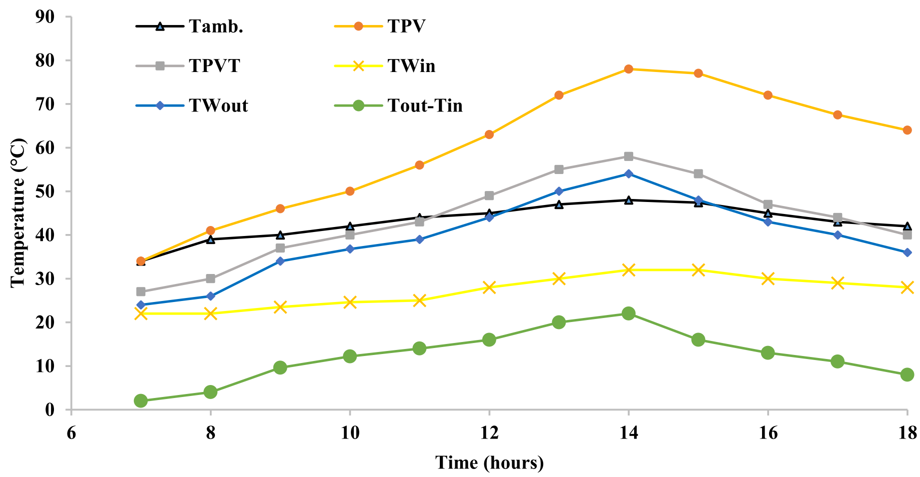

Figure 6. Average distribution of measured temperatures of the PVT system during the tests.

in Iraq (especially the central and southern cities, including Baghdad), which are characterized by high radiation intensity and high temperatures in summer. Figure 3 shows the measured values of the ambient temperatures are high and the solar radiation intensity is very high during the experiments period. The figure indicates that the average air temperature (for the period from 7 AM to 6 PM) was 43.73 °C, while the average radiation intensity (for the same pre-mentioned period) was 579.4 W/m^2. During the experimental period, the maximum achieved average ambient temperature was 49.22 °C, which was measured at 1:45 PM. Also, the maximum average radiation intensity measured was 833 W/m^2 which was measured in the time between 1:50 PM and 1:55 PM.

It was noted that the temperature of the soil changes as the measurements go deeper. It is high on the surface due to direct exposure to sunlight. Soil temperature goes down as the drilling is done in depth. Figure 4 shows the average soil temperatures measured during the study's 2 months. The

https://doi.org/10.1021/acsomega.2c07900
ACS Omega 2023, 8, 29926−29938

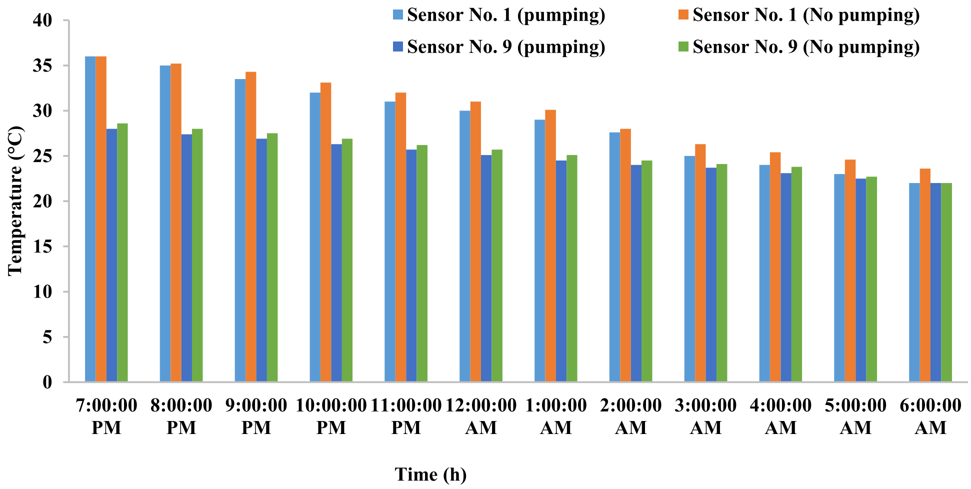

Figure 7. Average temperatures distributed over sensors during night.

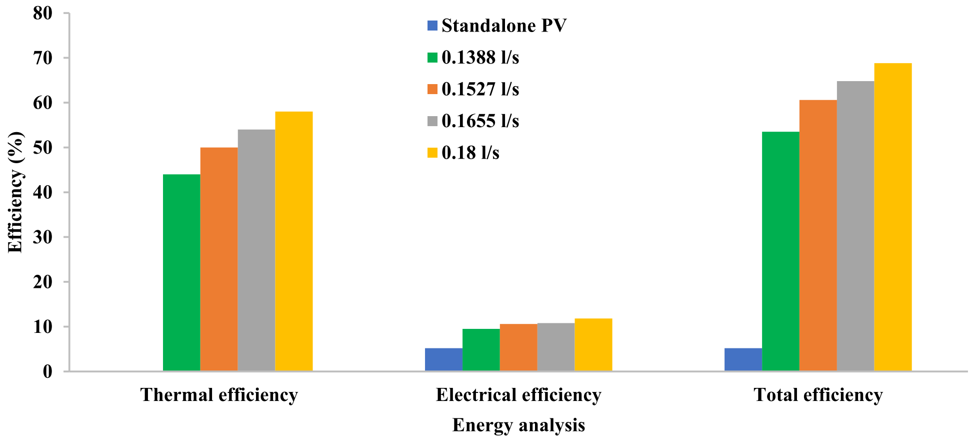

Figure 8. Average PVT system's efficiencies with flow rate variations.

surface temperatures of the study area were higher during the August by about 4 °C in comparison with July. This is normal, as the solar radiation intensity in August is higher than that of July. The average measured temperature reduced as the penetration takes place, reaching a temperature of 22.5 °C at a depth of 4 m below the surface of the earth. The difference between July and August measurements is present at other depths but disappears at this depth. This means that the effect of surface temperature does not affect it; thus, this depth selection for installing the UHE was appropriate. The results of the study are completely agreement with those of Majeed et al.[65]

Figure 5 shows the effect of water flow rate on its temperatures in the underground exchanger as measured by thermocouples distributed along the exchanger tube. At point 1, the water temperature is approximately equal and less than the water temperature coming from the PVT system due to the loss of a large part of the heat along the pipe (4 m depth). The higher the water volumetric flow rate, the lower its temperature at the end of UHE (points 8 and 9). The lowest temperature reached by the water at point 9 was 32 °C at 0.18 l/s flow rate; meanwhile, the water temperature at point 1 was 62 °C for the same flow rate.

This result shows the enormous potential of the soil to be a heat sink. The water temperature can be further reduced by increasing the flow rate that was determined (in recent study) to preserve the PVT system from vibrating. It is also possible to reach a water temperature equal to the temperature of the soil (22.5 °C) by increasing the length of the underground exchanger by several more meters. The main determinant of this increase is cost.

Figure 6 shows a summary of the different temperatures of the studied PVT system (above the earth's surface). It is observed that the maximum average air temperature (measured in the shade) was 48 °C, which is very far from the measured PV panel's surface temperatures. The surface of the standalone PV is completely exposed to solar radiation and the surrounding air which is much hotter than the ambient temperature due to exposure to the high solar radiation, which is an additional effect. The highest average surface temperature of PV reached 78 °C at 2 PM. The efficient cooling process causes a decrease of about 20 °C, bringing the average PV panel surface temperature of a PVT system to 58 °C at the same time. The Tout-Tin curve gives a direct indication of the heat transfer efficiency, as the difference was increased with the increase in the PVT system surface temperature, and the maximum average difference measured is at the highest temperatures of the PV surface. Therefore, higher PV module's temperature contributes to a more efficient cooling process, bringing the difference between the temperature of the inlet and outlet water at 2 PM to 22 °C. It is clear from Figure 6

https://doi.org/10.1021/acsomega.2c07900
ACS Omega 2023, 8, 29926−29938

that the measured T_{Win} levels are low. This difference improves the heat transfer and enhances the cooling process.

After sunset: PV panels stop generating electricity and the circulation of cooling water in the PVT system was also stopped. Figure 7 shows the process of heat dissipated in water (in buried pipes) for the period from 7 PM to 6 AM of the next day. During this period, heat is transferred by natural convection through water and from it to the tube wall and soil by thermal conduction. This process could be slow, but the length of time is sufficient to reach a thermal equilibrium between the exchanger and the soil. To summarize the findings from this study, the comparison was made in this figure between the average temperatures at points 1 and 9, which represent the first point of water entry and the last measurement point before it transfers to the earth surface. The measured readings show that the time it took for this process was sufficient for the water to reach the soil temperature. However, when considering a larger system with more panels, here it is better to forcibly circulate water to cool the system after the above-ground PVT systems stop. Consideration should also be given to measuring the rate of soil heat dissipation, which directly depends on its thermal conductivity.

The thermal, electrical, and overall efficiencies are usually calculated when studding PVT systems (Figure 8). Although in the current system, the thermal efficiency resulted from heat extracted from the PV panel was not utilized in any application but dissipated by the UHE. Thermal efficiency was calculated assuming the temperature of the water leaving the system for comparison purposes only. The standalone PV system electrical efficiency is very low in comparison with PVT system ones. Interestingly, this result explains the significant deterioration in the productivity of standalone PV module (5.2%) and insures the need for obtaining adequate cooling to recover some of their performance losses. It can be noticed that the electrical efficiency improved by increasing the flow rate of water in the PVT system, reaching its highest values of 11.82% at a flow rate of 0.18 l/s. This means an increase in electrical efficiency of up to 127.3% higher than standalone PV. This high improvement in electrical efficiency cannot be achieved without the participation of the GHE in cooling the circulated water.

Also, the thermal efficiency was raised by increasing flow rate as well. It is crucial to view the instantaneous electrical and thermal measurements to calculate the total efficiency of the PVT collector in addition to the peak achieved efficiency. However, it is better to evaluate the average efficiency corresponding to different operational parameters. Figure 8 shows the effect of water flow rate on the thermal, electrical, and total efficiency of the studied PVT system. The temperature of the water raised significantly during its passage through the heat exchanger of the PVT system and left the system with high temperatures, as shown in Figure 6. The heat gained by the water from the photovoltaic module was increased with its flow rate increase, which means an increase in the thermal efficiency of the system with a higher flow rate (0.18 l/s). Unfortunately, this efficiency is in fact is a wasted efficiency, as this heat is dissipated and disposed of by the UHE.

Figure 9 shows the exergy variance of the studied PV/T system. The figure represents the effect of the coolant flow rate on the thermal, electrical, and total exergies in the experiments. Tests were carried out at flow rates of 0.1388, 0.1527, 0.1655, and 0.18 l/s. The average obtained thermal exergies were 1.41, 0.67, 1.25, and 1.68%, respectively, compared to the standalone PV thermal exergy, which was 0.375%. Also, the electrical exergy of the PVT was in the range from 2.3 to 3.15% compared to 1.8 for the case of standalone PV module. The obtained results are consistent with the results of refs 77−7879. The figure also shows the total exergies of the PVT system, which was in the range of 2.97−4.83% compared to the standalone PV, which was 2.175%. This result is close to what was achieved by Nayak and Tiwari[80] who obtained a total exergy of 4% in a hybrid PVT application. The performance of the studied system was better than that tested by Sardarabadi et al.,[81] in which PV modules were cooled using multiple nanofluids. The calculated exergies were in the range of 1.77, 1.85, and 2.08%. Hosseinzadeh et al.[82] studied the exergy of a PVT system cooled with nanofluid and a phase change material, and the resulting exergy was in the range of 1.59 and 3.19%. Therefore, the cooling technology (using an underground) heat exchanger is an effective tool that results in an increase in the electrical power produced and a decrease in the energy lost.

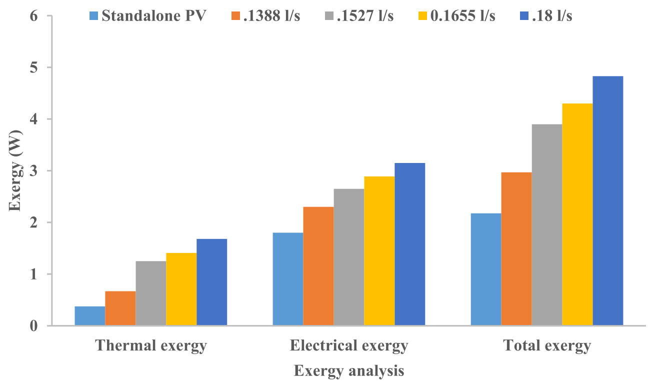

Figure 9. Average PVT system's exergies variations vs studied flow rates.

Table 2 compares the results from current study with results obtained from previous studies published in the literature that employed water to cool PVT systems. This comparison cannot be completely relied upon, as it may not be fair to the included studies because of the different types of PV modules used, weather conditions (radiation and temperature) and the type of exchanger used in the PVT system, as well as the collected heat dissipation method. Previous studies[82,85,86] and[13] had a high radiation intensity of 800 W/m^2 and more, as in the case of the current study, but the ambient temperatures were clearly lower. From reading the weather conditions of the rest of the studies, it turns out that the harshest natural weather conditions that were studied are in the current study. Also, the electrical efficiency achieved in this study is considered high and suitable despite these harsh atmospheric conditions. Some designs of the current study adopted some distinguished studies in the field of PVT systems and linking them to an appropriate underground cooling system, which is unprecedented in the Middle East and North Africa.

4. CONCLUSIONS

In this study, an UHEr was used to cool the circulating water in a PVT system installed in Baghdad-Iraq. The measurements were made in the most severe climate conditions during summer season (July and August 2022). In the beginning, it

https://doi.org/10.1021/acsomega.2c07900
ACS Omega 2023, 8, 29926−29938

Table 2. Comparison between the Results of Some Literature Studies and the Current Study

refs	electrical efficiency (%)	climate conditions: max. solar intensity (W/m^2)	climate conditions: max. ambient temperature (°C)	cooling fluid	collector type
Gomaa et al.[83]	9	1000	29	Water	Cross-fined channel box
Dubey and Tiwari[84]	9.5	850	38	Water	Flat plate
Ji et al.[85]	9.87	245.6	32.4	Water	Flat-box Al-alloy absorber plate
Chow et al.[86]	11	771	32.1	Water	Aluminum-alloy flat-box
Salem et al.[87]	13	800	35	Water	Aluminum channels
Kazem et al.[13]	9.3	880	38	Water	spiral flow
Shalaby et al.[88]	13	1087	43	Water	Direct flow
Menon et al.[89]	15	900	36	Water	serpentine copper pipes coil
Hasan et al.[90]	13.8	840	45	Water	Flat-box absorber plate
Kazem et al.[91]	10.8	773	37	Water	Web flow
Current study	11.82	833	49.22	Water	Spiral flow

was preparing the ground and reaching the appropriate depth for the installation of the UHE and its proper burial. Several measurements were made on the system and it was compared with the performance of the standing PV system. Soil temperatures decreased with greater depth to reach stability at 4 m depth and 22.5 °C. Also, the length of the UHE has a role in reducing the temperatures of the circulating water, as does the water volumetric flow rate. It was found that the best flow rate used to reach the best performance in the study was 0.18 l/s. It can be concluded that the large difference between exit water temperatures of the UHE (entering the PVT system) to increase the system's panel cooling efficiency. Furthermore, it was found that the standalone PV surface and PVT module's surface temperature deference was by about 20 °C. From studying the UHE temperatures after sunset, the heat dissipation process during at the night was efficient, as the temperature of the water in it reached a degree equal to the soil temperature. The electrical efficiency of the studied PVT system was higher than the standalone PV by 127.3%. In comparison of the results obtained in this study, which is the first of its kind in Middle East and North Africa, with other studies from the literature, it was observed that the system is feasible and efficient in such harsh weather conditions. In the future, it is suggested that the focus should be on the use of underground pipes with a long operational life. In addition, study the possibility of cooling a system consisting of a large number of PV panels from an engineering and system's cost point of view.

■ AUTHOR INFORMATION

Corresponding Author

Ahmed A. Al-Amiery − *Energy and Renewable Energies Technology Center, University of Technology—Iraq, Baghdad 10001, Iraq; Department of Chemical and Process Engineering, Faculty of Engineering and Built Environment, Universiti Kebangsaan Malaysia (UKM), Bangi 43000 Selangor, Malaysia;* orcid.org/0000-0003-1033-4904; Email: dr.ahmed1975@gmail.com, dr.ahmed1975@ukm.edu.my

Authors

Saif H. Majeed − *Mechanical Engineering Department, University of Technology—Iraq, Baghdad 10001, Iraq*

Amar S. Abdul-Zahra − *Mechanical Engineering Department, University of Technology—Iraq, Baghdad 10001, Iraq*

Dheya G. Mutasher − *Mechanical Engineering Department, University of Technology—Iraq, Baghdad 10001, Iraq*

Hayder A. Dhahd − *Mechanical Engineering Department, University of Technology—Iraq, Baghdad 10001, Iraq*

Mohammed A. Fayad − *Energy and Renewable Energies Technology Center, University of Technology—Iraq, Baghdad 10001, Iraq*

Ali H. A. Al-Waeli − *Engineering Department, American University of Iraq, Sulaimani, Sulaimani 46001, Iraq*

Hussein A. Kazem − *Faculty of Engineering, Sohar University, Sohar PCI 311, Oman*

Miqdam T. Chaichan − *Energy and Renewable Energies Technology Center, University of Technology—Iraq, Baghdad 10001, Iraq*

Wan Nor Roslam Wan Isahak − *Department of Chemical and Process Engineering, Faculty of Engineering and Built Environment, Universiti Kebangsaan Malaysia (UKM), Bangi 43000 Selangor, Malaysia;* orcid.org/0000-0002-1051-3120

Complete contact information is available at: https://pubs.acs.org/10.1021/acsomega.2c07900

Notes

The authors declare no competing financial interest.

■ ACKNOWLEDGMENTS

The authors extend their appreciation to the Universiti Kebangsaan Malaysia.

■ NOMENCLATURE

A_C	collector area (m^2)
A_{panel}	PV area (m^2)
E_f	primary energy (%)
$E_{x_{pv}}$	PV exergy (W)
$E_{x_{in}}$	exergy input (W)
E_{x_o}	exergy output (W)
E_{x_d}	exergy destruction (W)
$E_{x_{th}}$	thermal exergy (W)
E_{x_d}	PVT exergy (W)
I_s	solar irradiance $\left(\frac{W}{m^2}\right)$
I_{mp}	maximum power current (A)
$\dot{m}$	mass flow rate (kg/s)
N_c	number of cells
P_{mp}	maximum power output (W)
Q_u	heat gain (W)
T_i	inlet fluid (°C)

T_o outlet fluid (°C)
V_{mp} maximum power voltage (V)
η_{th} thermal efficiency (%)
η_e electrical efficiency of the PV (%)
η_{PVT} photovoltaic-thermal efficiency (%)
η_{PV} photovoltaic efficiency (%)

REFERENCES

(1) Al-Maamary, H. M.; Kazem, H. A.; Chaichan, M. T. Changing the energy profile of the GCC States: A review. *Int. J. Appl. Eng. Res.* **2016**, *11*, 1980−1988.

(2) Perera, F.; Nadeau, K. Climate Change, Fossil-Fuel Pollution, and Children's Health. *N. Engl. J. Med.* **2022**, *386*, 2303−2314.

(3) Goh, H. H.; Li, C.; Zhang, D.; Dai, W.; Lim, C. S.; Kurniawan, T. A.; Goh, K. C. Application of choosing by advantages to determine the optimal site for solar power plants. *Sci. Rep.* **2022**, *12*, 4113.

(4) Lamaamar, I.; Tilioua, A.; Hamdi Alaoui, M. A. H. Thermal performance analysis of a poly c-Si PV module under semi-arid conditions. *Mater. Sci. Energy Technol.* **2022**, *5*, 243−251.

(5) Martín-Chivelet, N.; Polo, J.; Sanz-Saiz, C.; Núñez Benítez, L. T.; Alonso-Abella, M.; Cuenca, J. Assessment of PV module temperature models for building-integrated photovoltaics (BIPV). *Sustainability* **2022**, *14*, 1500.

(6) Herrando, M.; Ramos, A. Photovoltaic-thermal (PV-T) systems for combined cooling, heating and power in buildings: A review. *Energies* **2022**, *15*, 3021.

(7) Hossain, F.; Karim, M. R.; Bhuiyan, A. A. A review on recent advancements of the usage of nano fluid in hybrid photovoltaic/thermal (PV/T) solar systems. *Renewable Energy* **2022**, *188*, 114−131.

(8) Elminshawy, A.; Morad, K.; Elminshawy, N. A. S.; Elhenawy, Y. Performance enhancement of concentrator photovoltaic systems using nanofluids. *Int. J. Energy Res.* **2021**, *45*, 2959−2979.

(9) Sornek, K.; Goryl, W.; Figaj, R.; Dąbrowska, G.; Brezdeń, J. Development and tests of the water cooling system dedicated to photovoltaic panels. *Energies* **2022**, *15*, 5884.

(10) Sangeetha, M.; Manigandan, S.; Chaichan, M. T.; Kumar, V. Progress of MWCNT, Al 2 O 3 , and CuO with water in enhancing the photovoltaic thermal system. *Int. J. Energy Res.* **2020**, *44*, 821−832.

(11) Elminshawy, N.; Elminshawy, A.; Osama, A.; Bassyouni, M.; Arıcı, M. Experimental performance analysis of enhanced concentrated photovoltaic utilizing various mass flow rates of Al2O3-nanofluid: Energy, exergy, and exergoeconomic study. *Sustain. Energy Technol. Assessments* **2022**, *53*, 102723.

(12) Hamzat, A. K.; Sahin, A. Z.; Omisanya, M. I.; Alhems, L. M. Advances in PV and PVT cooling technologies: A review. *Sustain. Energy Technol. Assessments* **2021**, *47*, 101360.

(13) Kazem, H. A.; Al-Waeli, A. H.; Chaichan, M. T.; Al-Waeli, K. H.; Al-Aasam, A. B.; Sopian, K. Evaluation and comparison of different flow configurations PVT systems in Oman: A numerical and experimental investigation. *Sol. Energy* **2020**, *208*, 58−88.

(14) Hou, G.; Taherian, H.; Song, Y.; Jiang, W.; Chen, D. A systematic review on optimal analysis of horizontal heat exchangers in ground source heat pump systems. *Renew. Sustain. Energy Rev.* **2022**, *154*, 111830.

(15) Liang, B.; Chen, M.; Orooji, Y. Effective parameters on the performance of ground heat exchangers: A review of latest advances. *Geothermics* **2022**, *98*, 102283.

(16) Mahmoud, M.; Alkhedher, M.; Ramadan, M.; Pullen, K.; Olabi, A. G.; Naher, S. Experimental investigation into the potential of using a shallow ground-cooled condenser in Lebanon. *Energy Convers. Manage.* **2022**, *264*, 115729.

(17) Zhou, K.; Mao, J.; Li, Y.; Zhang, H.; Chen, S.; Chen, F. Thermal and economic performance of horizontal ground source heat pump systems with different flowrate control methods. *J. Build. Eng.* **2022**, *53*, 104554.

(18) Soni, S. K.; Pandey, M.; Bartaria, V. N. Ground coupled heat exchangers: a review and applications. *Renew. Sustain. Energy Rev.* **2015**, *47*, 83−92.

(19) Renaud, T.; Verdin, P.; Falcone, G. Numerical simulation of a deep borehole heat exchanger in the Krafla geothermal system. *Int. J. Heat Mass Tran.* **2019**, *143*, 118496.

(20) Song, R.; Cui, M. Single- and multi-objective optimization of a plate-fin heat exchanger with offset strip fins adopting the genetic algorithm. *Appl. Therm. Eng.* **2019**, *159*, 113881.

(21) Cao, D.; Shi, B.; Zhu, H.-H.; Wei, G.; Bektursen, H.; Sun, M. A field study on the application of distributed temperature sensing technology in thermal response tests for borehole heat exchangers. *Bull. Eng. Geol. Environ.* **2019**, *78*, 3901−3915.

(22) Nicholson, S. R.; Kober, L. R.; Atefrad, P.; Mwesigye, A.; Dworkin, S. B. The influence of geometry on the performance of a helical steel pile as a geo-exchange system. *Renewable Energy* **2021**, *172*, 714−727.

(23) Ramos, R.; Aresti, L.; Yiannoukos, L.; Tsiolakis, E.; Pekris, J.; Vieira, A.; Florides, G.; Christodoulides, P. Thermal and physical characteristics of soils in Cyprus for use in shallow geothermal energy applications. *Energy, Ecol. Environ.* **2019**, *4*, 300−309.

(24) Naylor, S.; Ellett, K. M.; Gustin, A. R. Spatiotemporal variability of ground thermal properties in glacial sediments and implications for horizontal ground heat exchanger design. *Renewable Energy* **2015**, *81*, 21−30.

(25) Liang, B.; Chen, M.; Fu, B.; Li, H. Investigation on the thermal and flow performances of a vertical spiral-tube ground heat exchanger in sand combined with kaolin additive. *Energy Build.* **2019**, *190*, 235−245.

(26) Li, W.; Li, X.; Peng, Y.; Wang, Y.; Tu, J. Experimental and numerical studies on the thermal performance of ground heat exchangers in a layered subsurface with groundwater. *Renewable Energy* **2020**, *147*, 620−629.

(27) Hassanzadeh, R.; Darvishyadegari, M.; Arman, S. A new idea for improving the horizontal straight ground source heat exchangers performance. *Sustain. Energy Technol. Assessments* **2018**, *25*, 138−145.

(28) Javadi, H.; Mousavi Ajarostaghi, S. S.; Rosen, M. A.; Pourfallah, M. Performance of ground heat exchangers: a comprehensive review of recent advances. *Energy* **2019**, *178*, 207−233.

(29) Hou, G.; Taherian, H.; Song, Y.; Jiang, W.; Chen, D. A systematic review on optimal analysis of horizontal heat exchangers in ground source heat pump systems. *Renew. Sustain. Energy Rev.* **2022**, *154*, 111830.

(30) Banerjee, A.; Chakraborty, T.; Matsagar, V. Evaluation of possibilities in geothermal energy extraction from oceanic crust using offshore wind turbine monopiles. *Renew. Sustain. Energy Rev.* **2018**, *92*, 685−700.

(31) Noorollahi, Y.; Saeidi, R.; Mohammadi, M.; Amiri, A.; Hosseinzadeh, M. The effects of ground heat exchanger parameters changes on geothermal heat pump performance - A review. *Appl. Therm. Eng.* **2018**, *129*, 1645−1658.

(32) Agrawal, K. K.; Misra, R.; Agrawal, G. Improving the thermal performance of ground air heat exchanger system using sand-bentonite (in dry and wet condition) as backfilling material. *Renewable Energy* **2019**, *146*, 2008−2023.

(33) Faizal, M.; Bouazza, A.; Singh, R. M. Heat transfer enhancement of geothermal energy piles. *Renew. Sustain. Energy Rev.* **2016**, *57*, 16−33.

(34) Tang, F.; Nowamooz, H. Outlet temperatures of a slinky-type horizontal ground heat exchanger with the atmosphere-soil interaction. *Renewable Energy* **2020**, *146*, 705−718.

(35) Jia, G. S.; Tao, Z. Y.; Meng, X. Z.; Ma, C. F.; Chai, J. C.; Jin, L. W. Review of effective thermal conductivity models of rock-soil for geothermal energy applications. *Geothermics* **2019**, *77*, 1−11.

(36) Wang, Z.; Wang, F.; Liu, J.; Li, Y.; Wang, M.; Luo, Y.; Ma, L.; Zhu, C.; Cai, W. Energy analysis and performance assessment of a hybrid deep borehole heat exchanger heating system with direct heating and coupled heat pump approaches. *Energy Convers. Manage.* **2023**, *276*, 116484.

(37) Cao, S.-J.; Kong, X.-R.; Deng, Y.; Zhang, W.; Yang, L.; Ye, Z.-P. Investigation on thermal performance of steel heat exchanger for ground source heat pump systems using full-scale experiments and numerical simulations. *Appl. Therm. Eng.* **2017**, *115*, 91−98.
(38) Ren, C.; Deng, Y.; Cao, S.-J. Evaluation of polyethylene and steel heat exchangers of ground source heat pump systems based on seasonal performance comparison and life cycle assessment. *Energy Build.* **2018**, *162*, 54−64.
(39) Wan, R.; Chen, M. Q.; Huang, Y. W.; Zhou, T.; Liang, B.; Luo, H. Evaluation on the heat transfer performance of a vertical ground U-shaped tube heat exchanger buried in soil-polyacrylamide. *Exp. Heat Tran.* **2017**, *30*, 427−440.
(40) Zhao, Q.; Chen, B.; Liu, F. Study on the thermal performance of several types of energy pile ground heat exchangers: U-shaped, W-shaped and spiral-shaped. *Energy Build.* **2016**, *133*, 335−344.
(41) Boughanmi, H.; Lazaar, M.; Farhat, A.; Guizani, A. Evaluation of soil thermal potential under Tunisian climate using a new conic basket geothermal heat exchanger: Energy and exergy analysis. *Appl. Therm. Eng.* **2017**, *113*, 912−925.
(42) Brunetti, G.; Saito, H.; Saito, T.; Šimůnek, J. A computationally efficient pseudo-3D model for the numerical analysis of borehole heat exchangers. *Appl. Energy* **2017**, *208*, 1113−1127.
(43) Dehghan, B. Effectiveness of using spiral ground heat exchangers in ground source heat pump system of a building for district heating/cooling purposes: comparison among different configurations. *Appl. Therm. Eng.* **2018**, *130*, 1489−1506.
(44) Cao, S.-J.; Kong, X.-R.; Deng, Y.; Zhang, W.; Yang, L.; Ye, Z.-P. Investigation on thermal performance of steel heat exchanger for ground source heat pump systems using full-scale experiments and numerical simulations. *Appl. Therm. Eng.* **2017**, *115*, 91−98.
(45) Ren, C.; Deng, Y.; Cao, S.-J. Evaluation of polyethylene and steel heat exchangers of ground source heat pump systems based on seasonal performance comparison and life cycle assessment. *Energy Build.* **2018**, *162*, 54−64.
(46) Bina, S. M.; Fujii, H.; Tsuya, S.; Kosukegawa, H. Comparative study of hybrid ground source heat pump in cooling and heating dominant climates. *Energy Convers. Manage.* **2022**, *252*, 115122.
(47) Lyu, C.; Leong, W. H.; Zheng, M.; Jiang, P.; Yu, F.; Liu, Y. Dynamic simulation and operating characteristics of ground-coupled heat pump with solar seasonal heat storage system. *Heat Transfer Eng.* **2020**, *41*, 840−850.
(48) Mousa, M. M.; Bayomy, A. M.; Saghir, M. Z. Long-term performance investigation of a GSHP with actual size energy pile with PCM. *Appl. Therm. Eng.* **2022**, *210*, 118381.
(49) Yoon, S.; Kim, M.-J.; Jeon, J.-S.; Jung, Y.-B. Significance evaluation of performance factors on horizontal spiral-coil ground heat exchangers. *J. Build. Eng.* **2021**, *35*, 102044.
(50) Zhou, K.; Mao, J.; Zhang, H.; Li, Y.; Yu, X.; Chen, F.; Li, M. Design strategy and techno-economic optimization for hybrid ground heat exchangers of ground source heat pump system. *Sustain. Energy Technol. Assessments* **2022**, *52*, 102140.
(51) Zhou, C.; Zarrella, A.; Yao, Y.; Ni, L. Analysis of the effect of icing on the thermal behavior of helical coil heat exchangers in surface water heat pump applications. *Int. J. Heat Mass Transfer* **2022**, *183*, 122074.
(52) Jahanbin, A. Thermal performance of the vertical ground heat exchanger with a novel elliptical single U-tube. *Geothermics* **2020**, *86*, 101804.
(53) Serageldin, A. A.; Radwan, A.; Katsura, T.; Sakata, Y.; Nagasaka, S.; Nagano, K. Parametric analysis, response surface, sensitivity analysis, and optimization of a novel spiral-double ground heat exchanger. *Energy Convers. Manag.* **2021**, *240*, 114251.
(54) Zhou, K.; Mao, J.; Li, Y.; Xiang, J. Parameters optimization of borehole and internal thermal resistance for single U-tube ground heat exchangers using Taguchi method. *Energy Convers. Manag.* **2019**, *201*, 112177.
(55) Liu, Z.; Xu, K.; Zhang, Q.; Yang, M. Numerical simulation on the heat recovery law of exploiting geothermal energy from a closed-loop geothermal system converted from an abandoned five-spot well pattern. *ACS Omega* **2022**, *7*, 41723−41731.
(56) Meng, X.; Han, Z.; Hu, H.; Zhang, H.; Li, X. Studies on the performance of ground source heat pump affected by soil freezing under groundwater seepage. *J. Build. Eng.* **2021**, *33*, 101632.
(57) Choudhary, K.; Jakhar, S.; Gakkhar, N.; Sangwan, K. S. Comparative life cycle assessments of photovoltaic thermal systems with earth water heat exchanger cooling. *Procedia CIRP* **2022**, *105*, 255−260.
(58) Ruoping, Y.; Xiangru, Y.; Xiaohui, Y.; Yunpeng, B.; Huajun, W. Performance study of split type ground source heat pump systems combining with solar photovoltaic-thermal modules for rural households in North China. *Energy Build.* **2021**, *249*, 111190.
(59) Sommerfeldt, N.; Madani, H. Review of solar PV/thermal plus ground source heat pump systems for European multi-family houses. In *11th ISES Eurosun Conference*; Palma de Mallorca: Spain, 2016; pp 1382−1393.
(60) Alnasser, T. M. A.; Mahdy, A. M. J.; Abass, K. I.; Chaichan, M. T.; Kazem, H. A. Impact of dust ingredient on photovoltaic performance: An experimental study. *Sol. Energy* **2020**, *195*, 651−659.
(61) Yin, H.; Zhang, C.; Zhou, X.; Chen, T.; Dong, F.; Cheng, W.; Tang, R.; Xu, G.; Jiao, P. Research on the Genetic Mechanism of High-Temperature Groundwater in the Geothermal Anomalous Area of Gold Deposit−Application to the Copper Mine Area of Yinan Gold Mine. *ACS Omega* **2022**, *7*, 43231−43241.
(62) Adamo, N.; Al-Ansari, N.; Sissakian, V.; Jehad Fahmi, K.; Ali Abed, S. Climate change: Droughts and increasing desertification in the Middle East, with special reference to Iraq. *Engineering* **2022**, *14*, 235−273.
(63) Chaichan, M. T.; Kazem, H. A.; Alnaser, N. W.; Gholami, A.; Al-Waeli, A. H.; Alnaser, W. E. Assessment cooling of photovoltaic modules using underground water. *Arab. Gulf J. Sci. Res.* **2022**, *39*, 151−169.
(64) Chaichan, M. T.; Kazem, H. A. Experimental evaluation of dust composition impact on photovoltaic performance in Iraq. *Energy Sources, Part A* **2020**, 1−22.
(65) Majeed, S. H.; Abdul-Zahra, A. S.; Mutasher, D. G. Performance evaluation of different types of ground source heat exchangers in a hot and dry climate. *Heat Transfer* **2022**, *51*, 5700−5722.
(66) Kazem, H. A.; Al-Waeli, A. H.; Chaichan, M. T.; Al-Waeli, K. H.; Al-Aasam, A. B.; Sopian, K. Evaluation and comparison of different flow configurations PVT systems in Oman: A numerical and experimental investigation. *Sol. Energy* **2020**, *208*, 58−88.
(67) Al-Smairan, M. Application of photovoltaic array for pumping water as an alternative to diesel engines in Jordan Badia, Tall Hassan station: Case study. *Renew. Sustain. Energy Rev.* **2012**, *16*, 4500−4507.
(68) Kazem, H. A.; Khatib, T.; Sopian, K. Sizing of a standalone photovoltaic/battery system at minimum cost for remote housing electrification in Sohar, Oman. *Energy Build.* **2013**, *61*, 108−115.
(69) *Heat Transfer*, 10th ed.; Holman, J., Ed.; McGraw Hill Higher Education, 2010.
(70) Niyas, H.; Prasad, S.; Muthukumar, P. Performance investigation of a lab-scale latent heat storage prototype - Numerical results. *Energy Convers. Manage.* **2017**, *135*, 188−199.
(71) Qi, C.; Li, C.; Li, K.; Han, D. Natural convection of nanofluids in solar energy collectors based on a two-phase lattice Boltzmann model. *J. Therm. Anal. Calorim.* **2021**, *147*, 2417−2438.
(72) Huang, J.; Wang, X.; Long, Q.; Wen, X.; Zhou, Y.; Li, L. Influence of pH on the stability characteristics of nanofluids. In *Proceedings of the 2009 Symposium Photonics Optoelectron*, SOPO, Wuhan, China, 14−16 August 2009; 2−4. DOI: 10.1109/SOPO.2009.5230102.
(73) Li, X.; Zhu, D.; Wang, X. Evaluation on dispersion behavior of the aqueous copper nano-suspensions. *J. Colloid Interface Sci.* **2007**, *310*, 456−463.
(74) Utomo, A. T.; Poth, H.; Robbins, P. T.; Pacek, A. W. Experimental and theoretical studies of thermal conductivity, viscosity

and heat transfer coefficient of titania and alumina nanofluids. *Int. J. Heat Mass Tran.* **2012**, *55*, 7772−7781.
(75) Cacua, K.; Ordoñez, F.; Zapata, C.; Herrera, B.; Pabón, E.; Buitrago-Sierra, R. Surfactant concentration and pH effects on the zeta potential values of alumina nanofluids to inspect stability. *Colloids Surf., A* **2019**, *583*, 123960.
(76) Suganthi, K. S.; Rajan, K. S. Temperature induced changes in ZnO-water nanofluid: Zeta potential, size distribution and viscosity profiles. *Int. J. Heat Mass Tran.* **2012**, *55*, 7969−7980.
(77) Mugi, V. R.; Chandramohan, V. P. Energy and exergy analysis of forced and natural convection indirect solar dryers: Estimation of exergy inflow, outflow, losses, exergy efficiencies and sustainability indicators from drying experiments. *J. Clean. Prod.* **2021**, *282*, 124421.
(78) Abdelkader, T. K.; Zhang, Y.; Gaballah, E. S.; Wang, S.; Wan, Q.; Fan, Q. Energy and exergy analysis of a flat-plate solar air heater coated with carbon nanotubes and cupric oxide nanoparticles embedded in black paint. *J. Clean. Prod.* **2020**, *250*, 119501.
(79) Abuşka, M.; Şevik, S. Energy, exergy, economic and environmental (4E) analyses of flat-plate and V-groove solar air collectors based on aluminum and copper. *Sol. Energy* **2017**, *158*, 259−277.
(80) Nayak, S.; Tiwari, G. N. Energy and exergy analysis of photovoltaic/thermal integrated with a solar greenhouse. *Energy Build.* **2008**, *40*, 2015−2021.
(81) Sardarabadi, M.; Hosseinzadeh, M.; Kazemian, A.; Passandideh-Fard, M. Experimental investigation of the effects of using metal-oxides/water nanofluids on a photovoltaic thermal system (PVT) from energy and exergy viewpoints. *Energy* **2017**, *138*, 682−695.
(82) Hosseinzadeh, M.; Sardarabadi, M.; Passandideh-Fard, M. Energy and exergy analysis of nanofluid based photovoltaic thermal system integrated with phase change material. *Energy* **2018**, *147*, 636−647.
(83) Gomaa, M. R.; Ahmed, M.; Rezk, H. Temperature distribution modeling of PV and cooling water PV/T collectors through thin and thick cooling cross-fined channel box. *Energy Rep.* **2022**, *8*, 1144−1153.
(84) Dubey, S.; Tiwari, G. N. Analysis of PV/T flat plate water collectors connected in series. *Sol. Energy* **2009**, *83*, 1485−1498.
(85) Ji, J.; Lu, J. P.; Chow, T. T.; He, W.; Pei, G. A sensitivity study of a hybrid photovoltaic/thermal water-heating system with natural circulation. *Appl. Energy* **2007**, *84*, 222−237.
(86) Chow, T. T.; Ji, J.; He, W. Photovoltaic-Thermal Collector System for Domestic Application. *J. Sol. Energy Eng.* **2007**, *129*, 205−209.
(87) Salem, M. R.; Elsayed, M. M.; Abd-Elaziz, A. A.; Elshazly, K. M. Performance enhancement of the photovoltaic cells using Al2O3/PCM mixture and/or water cooling-techniques. *Renewable Energy* **2019**, *138*, 876−890.
(88) Shalaby, S. M.; Elfakharany, M. K.; Moharram, B. M.; Abosheiasha, H. F. Experimental study on the performance of PV with water cooling. *Energy Rep.* **2022**, *8*, 957−961.
(89) Menon, G. S.; Murali, S.; Elias, J.; Aniesrani Delfiya, D. A.; Alfiya, P. V.; Samuel, M. P. Experimental investigations on unglazed photovoltaic-thermal (PVT) system using water and nanofluid cooling medium. *Renewable Energy* **2022**, *188*, 986−996.
(90) Hasan, H. A.; Sherza, J. S.; Mahdi, J. M.; Togun, H.; Abed, A. M.; Ibrahim, R. K.; Yaïci, W. Experimental evaluation of the thermoelectrical performance of photovoltaic-thermal systems with a water-cooled heat sink. *Sustainability* **2022**, *14*, 10231.
(91) Kazem, H. A.; Al-Waeli, A. H.; Chaichan, M. T.; Sopian, K. Numerical and experimental evaluation of nanofluids based photovoltaic/thermal systems in Oman: Using silicone-carbide nanoparticles with water-ethylene glycol mixture. *Case Stud. Therm. Eng.* **2021**, *26*, 101009.